Int. J. Electrochem. Sci., 13 **(2018)** 915 – 924, doi: 10.20964/2018.01.52

International Journal of
ELECTROCHEMICAL
SCIENCE
www.electrochemsci.org

Short Communication

The Effect of Temperature on the Hydrogen Permeation of Pipeline Steel in Wet Hydrogen Sulfide Environments

Zhu Wang[1], *Mingliang Liu*[1, 2], *Minxu Lu*[1, *], *Lei Zhang*[1], *Junyan Sun*[1], *Ziru Zhang*[1], *Xian Tang*[1]

[1] Institute for Advanced Materials and Technology, University of Science and Technology Beijing, Beijing 100083, PR China
[2] Baoshan Iron & Steel Co., Ltd., 201900, PR China
[*]E-mail: Lumx@ustb.edu.cn

Received: 23 September 2017 / *Accepted:* 12 November 2017 / *Published:* 16 December 2017

In this study, the effect of temperature on the hydrogen permeation of pipeline steel in wet H_2S environments was studied. The steady-state permeation current density, steady-state flux, and the permeation rate increased with increasing temperature. The corrosion rate increased at 35^{o}C and was confirmed by the electrochemical tests. The result of this study indicated that the corrosion process was controlled by the cathodic reaction. The hydrogen permeation behavior ~~in~~ under wet H_2S condition was affected by the corrosion rate and the corrosion product.

Keywords: pipeline steel, hydrogen sulfide, temperature, hydrogen permeation

1. INTRODUCTION

Pipeline steel has been widely used in the oil and gas fields owing to its high strength and low cost. In most cases, the presence of H_2S in aqueous solution can significantly decrease the corrosion resistance of pipeline steels. Electrochemical reactions and the formation of iron sulfides are the two major factors of significance for H_2S corrosion [1]. H_2S corrosion has been extensively studied with respect to factors such as pH, H_2S concentration, and temperature [2]. In general, the presence of H_2S can either promote or inhibit the corrosion rate of carbon steels, depending on the partial pressure of H_2S [3].

Moreover, the presence of H_2S can also promote the hydrogen charging in the steel and thus increase the risk of hydrogen embrittlement [4]. Some failures accidents, which are caused by the H_2S-induced hydrogen embrittlement, have been reported in recent years.[5, 6] Zhou [7, 8] conducted the hydrogen permeation tests in H_2S-containing solution and found that the amount of diffusible

hydrogen significantly increased with increasing P_{H2S} and hydrogen permeation is dependent on the formation of the corrosion scale. However, there are only few reports on the creaking of pipeline steel in wet H_2S-containing condition.

In this study, the effect of temperature on the hydrogen permeation of pipeline steel in wet hydrogen sulfide environments was studied. Hydrogen was directly generated on the sample surface by the H_2S corrosion reaction rather than by the cathodic polarization. The corrosion rate under wet H_2S condition was evaluated by the weight loss and electrochemical tests. The permeation behavior was illustrated by the corrosion rate and the protectiveness of corrosion products.

2. EXPERIMENTAL

2.1 Materials and sample preparation

The experimental material was commercial X52 pipeline steel with the microstructure of typical ferrite and pearlite. The chemical composition of X52 is listed in Table 1. The specimens for the hydrogen permeation experiments were 55-mm-diameter plates with a thickness of 0.7 mm. The plates were then subsequently ground with 300, 600, 800, and 1200 grit silicon carbide paper. Specimens (10 mm ×10 mm× 3 mm) for the wet H_2S corrosion tests were pre-treated in a manner similar to the permeation specimens. All the specimens were cleaned with deionized water, degreased in acetone, and dried in alcohol under cold air.

Table 1. Chemical Composition of X52 Pipeline Steel (wt. %)

C	Si	Mn	S	P	Mo	V	Fe
0.11	0.27	1.10	0.0032	0.006	0.003	≤0.01	Bal.

2.2. Electrochemical hydrogen permeation test

The hydrogen permeation test was conducted in a developed Devanathan−Stachurski hydrogen permeation device, as shown in Fig. 1. The cell was composed of two compartments, a hydrogen generating cell and a hydrogen oxidizing cell. The detection side of the specimen was deposited with a nickel film in Watt's bath of 250 g/L $NiSO_4 \cdot 7H_2O$ + 45 g/L $NiCl_2 \cdot 6H_2O$ +40 g/L H_3BO_3 using a cathodic current density of 10 mA/cm^2. The detection side was held at 300 mV (vs. SCE) in 0.2 mol/L NaOH solution, under which the steel was considered to be at a passive potential.

Deionized water was filled at the bottom of the input side to make wet gas environment, and then the input side was deoxygenated by pure N_2 for 8 h. The testing system was then set to the required temperature. When the background oxidation current density is less than 1 μA/cm^2, H_2S gas should be introduced, and the oxidation current density will be continuously recorded.

Prior to the hydrogen permeation tests, the original weight of each specimen was measured by an analytical balance with an accuracy of 10^{-4} g. After the experiments, the corroded specimens were extracted and immediately rinsed with absolute ethyl alcohol. The corrosion products were removed according to ASTM G1-03 standard, then rinsed, dried, and reweighed to obtain the final weight of the specimen. The corrosion rate was calculated by the following equation:

$$r_{\mathrm{corr}} = \frac{8.76 \times 10^{4} \times \left(m - m_{\mathrm{t}}\right)}{S \times t \times \rho}$$

where r_{corr} is the corrosion rate, mm/a; m and m_{t} are the original and final weights of the specimens, respectively, g; S is the exposed surface area, cm^2; ρ is the steel density, g/cm^2; and t represents the immersion time, h.

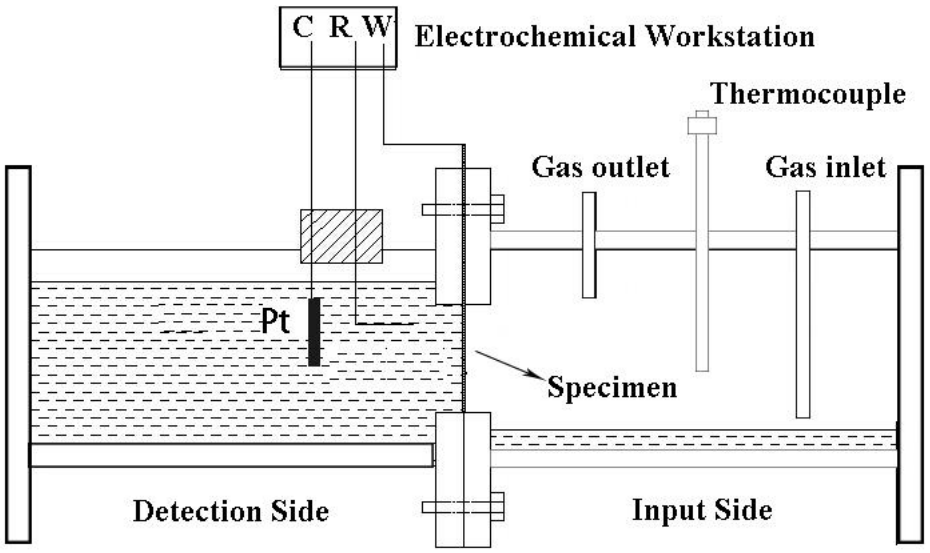

Figure 1. Schematic for hydrogen permeation device in wet H_2S environment

2.3. Corrosion tests

Corrosion tests were conducted in a specially designed vessel to simulate the wet gas corrosion. The vessel was similar to the hydrogen permeation device. The specimens with the size of 10 mm ×10 mm× 3 mm were fixed in the left side of the input side. Deionized water was transferred and then deoxygenated by pure N_2 for 8 h. H_2S was gradually introduced and continuously bubbled. The corrosion time was consistent with the electrochemical hydrogen permeation test. The removed samples after the tests were cleaned with distilled water and dried with cold air.

The above pre-corroded specimens were then analyzed by electrochemical tests, X-ray diffraction (XRD, Cu Ka, k = 0.154 nm, Rigaku), and scanning electron microscopy (SEM, LEO-1450).

2.4. Electrochemical tests

Potentiodynamic polarization measurements were conducted at 22°C in a naturally aerated 3.5% NaCl aqueous solution on the pre-corroded specimens as described in Section 2.3. The counter electrode was a platinum plate with a surface area of 4 cm^2 and the reference electrode was a saturated calomel electrode (SCE). Potentiodynamic polarization curves were obtained at a potential scan rate of 0.5 mV/s. The potential range was from −0.20 V to 0.50 V vs. open-circuit potential (OCP).

3. RESULTS AND DISCUSSION

3.1 Hydrogen permeation

The hydrogen permeation curves of X52 pipeline steel in wet hydrogen sulfide environment at various temperatures are shown in Fig. 2.

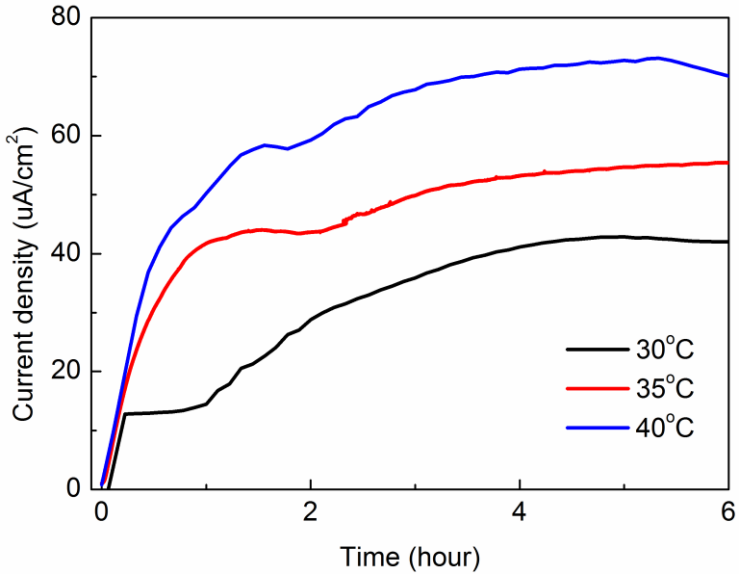

Figure 2. Hydrogen permeation curves of X52 pipeline steel in wet H_2S environment at various temperatures at a partial H_2S pressure of 0.1 MPa.

The oxidation current density increased significantly when H_2S was introduced, and the permeation curves became stable about 4 h later. The flux of hydrogen through the specimen was measured in terms of the current density i_p, and converted to the hydrogen permeation flux according to the following equation:

$J_\infty = i_p^\infty / nF$

where J_∞ is the steady-state flux, i_p^∞ is the steady-state permeation current density, n is the number of electrons transferred, and F is Faraday's constant.

The permeation rate (φ) is defined by:

$\varphi = J_\infty L = i_p^\infty L / nF$

where L is the specimen thickness.

The effective diffusion coefficient (D_{eff}) was calculated by the time-lag method:

$D_{eff}=L^2/(6t_{0.63})$

where $t_{0.63}$ is the lag time to achieve a permeation flux of 63% J_∞.

The calculated permeation data of X52 are listed in Table 2. As the temperature increased from 30 to 40°C, the steady-state permeation current density increased from 42.84 μA/cm^2 to 55.44 and 72.35 μA/cm^2, respectively.

The steady-state flux and the permeation rate also increased with temperature, indicating that more hydrogen atoms diffused to the specimens with increasing temperature. This result was correlated with the corrosion rates and properties of corrosion scale. According to the principles of electrochemistry of corrosion, the anodic corrosion rate equals the cathodic corrosion rate. Thus, a higher corrosion rate means a larger number of hydrogen atoms generated on the sample surface. Meanwhile, corrosion scale can significantly affect the corrosion process, acting as a diffusion barrier for hydrogen atoms.

Table 2. Hydrogen permeation parameters of X52 pipeline steel in wet H_2S environment at various temperatures at a partial H_2S pressure of 0.1 MPa.

T, °C	D_{eff}, ×10^{-7}cm^2/s	i_∞, μA/cm^2	J_∞, ×10^{-11}mol/cm^2/s	φ, ×10^{-11}mol/s/cm
30	2.91	42.84	44.39	2.22
35	3.66	55.44	57.45	2.87
40	1.19	72.35	74.97	4.50

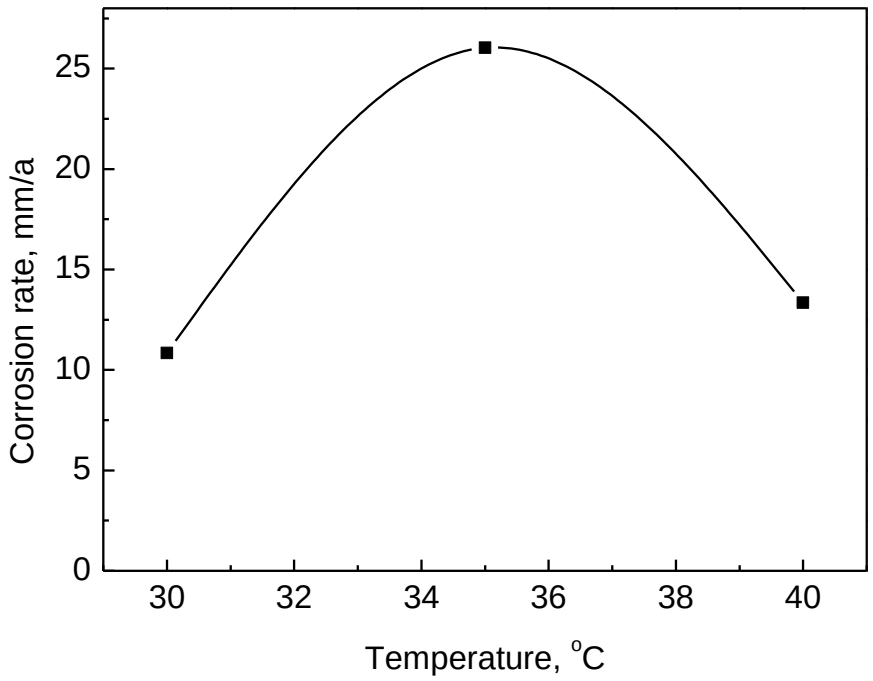

Figure 3. Corrosion rate of hydrogen permeation specimens at various temperatures at a partial H_2S pressure of 0.1 MPa.

The corrosion rate curve of the permeation specimens was plotted in Fig. 3. It is noteworthy that the corrosion rate at 40°C was higher than that at 30°C, and reached the peak value at 35°C. This result was consistent with the result of Zhou [8], who assumed that the higher corrosion rate at 35°C was attributed to the competitive effect of the interfacial reaction and the corrosion scale. They thought that at temperatures <35°C the corrosion products were less protective. Therefore, the corrosion rate increased with temperature. However, at temperatures >50°C, the protective property of the corrosion scale is greatly improved. As a result, the corrosion rates at 35°C are higher than those at other temperatures. The reason for the maximum corrosion rate at 35°C in wet H_2S environment was investigated by electrochemical tests.

3.2 Potentiodynamic polarization measurement

Fig.4 shows the potentiodynamic polarization curves of the corroded specimens measured in a naturally aerated 3.5% NaCl aqueous solution at 22°C. The anodic branches were similar for all the specimens, whereas the cathodic branches were quite different. This result indicated the corrosion process was under the control of the cathodic reaction. Some researches demonstrated that the similarity of anodic branches was related to metal dissolution.[9-11], indicating that the corrosion scales formed on the sample surface is not protective enough. The difference in the cathodic current densities was caused by the corrosion product film formed in wet H_2S environment. The electrochemical corrosion parameters, namely corrosion potential (E_{corr}), anodic and cathodic Tafel slopes (β_a, β_c) and corrosion current density (I_{corr}) obtained by extrapolation of the Tafel lines are listed in Table 3. As is seen, E_{corr} at 35°C was approximately 100 mV more positive than that measured at 30 and 40°C. This was attributed to the denser corrosion scale formed at 35°C (see SEM images below in Fig. 5). β_a values were nearly the same under three conditions, while β_c value was significantly lower at 35°C, indicating its hydrogen evolution was more favorable. Due to the corrosion process was under the control of cathodic reaction, the corrosion current density was the highest at 35°C.

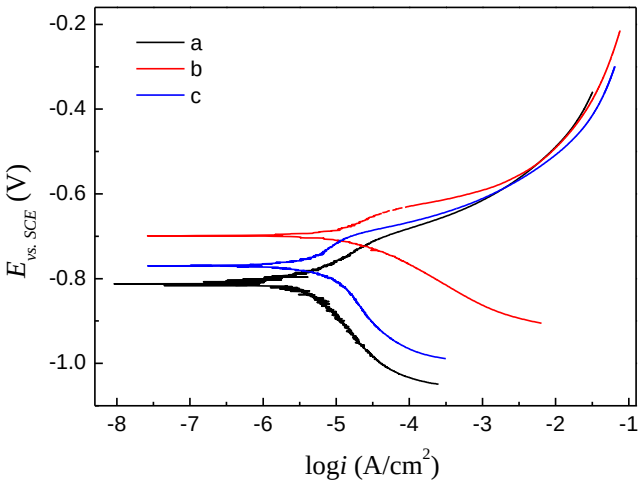

Figure 4. Potentiodynamic polarization curves of specimens pre-corroded in wet H_2S environment at various temperatures: (a) pre-corroded at 30°C; (b) pre-corroded at 35°C; (c) pre-corroded at 40°C. The curves are measured in a naturally aerated 3.5% NaCl aqueous solution at 22°C.

Table 3. Corrosion parameters obtained from potentiodynamic polarization curves: (a) pre-corroded at 30°C; (b) pre-corroded at 35°C; (c) pre-corroded at 40°C

Situation	E_{corr}, V	β_a, V dec^{-1}	β_c, V dec^{-1}	I_{corr}, μA cm^{-2}
a	–0.81	0.06	0.15	4.37
b	–0.70	0.05	0.11	26.21
c	–0.77	0.05	0.15	22.57

As discussed by the electrochemical tests, the corrosion product film did not contribute much to the protective effect. The corrosion process of carbon steel in wet H_2S environment was mainly controlled by the cathodic reaction. Therefore, the corrosion process could be described by the following reactions: [12, 13]

$Fe \rightarrow Fe^{2+} + 2e$

$H_2S + H_2O \rightarrow H_3O^+ + HS^-$

$HS^- + H_2O \rightarrow H_3O^+ + S^{2-}$

$H_3O^+ + e \rightarrow H_{ads} + H_2O$

$2H_{ads} \rightarrow H_2$ and $H_{ads} \rightarrow H_{metal}$

In wet H_2S environment, H_2S gas is dissolved in the condensed water, releasing hydrogen ions. Hydrogen ions suffered a charge transfer step to produce adsorbed hydrogen atoms. Two adsorbed hydrogen atoms combined to produce a hydrogen molecule. Simultaneously, the atomic hydrogen entered into the steel from the surface adsorbed state in parallel with the desorption reaction. It has been shown [14] that lattice defects (vacancies, dislocations, grain boundaries) provide a variety of trapping sites. Hydrogen traps are mechanistically classified as reversible and irreversible [15], depending on the steepness of the energy barrier needed to be overcome by hydrogen to escape from them. Meanwhile, iron continuously oxidized into Fe^{2+}. When the concentrations of Fe^{2+} and S^{2-} ions exceeded the solubility limit, corrosion products participated.

For hydrogen permeation tests, no potential was applied in the hydrogen generating cell. The specimens suffered anodic iron dissolution and cathodic hydrogen evolution process simultaneously. The number of generated hydrogen atoms was only proportional to the corrosion rates. However, the deposition of the corrosion products can significantly affect the hydrogen permeation process from two aspects. On one hand, deposited iron sulfide will change the position of hydrogen evolution. As is well acknowledged, the potential of the corrosion products was always more positive than that of the bare steel. Moreover, iron sulfide was thought to be a type of semiconductor. These make iron sulfide a natural cathode. On the other hand, corrosion products acted as the barrier for hydrogen permeation, which somewhat inhibited because of the hindering effect of corrosion products.

The number of generated hydrogen atoms is calculated according to the following equation:

$$H_{total} = \frac{2 \times m_{WL}}{M_{Fe}}$$

where H_{total} is the total number of generated hydrogen atoms in mol, m_{WL} is the weight loss in g, M_{Fe} is the molar mass, in g/mol.

The rate of hydrogen generating was calculated by the following equation:

$$J_{total}=\frac{H_{total}}{A \times t}$$

where J_{total} is the rate of hydrogen generated on the sample surface in mol/cm^2/s, A is the exposed surface area of the specimens, and t represents the time for H_2S bubbling.

Table 4. The calculated hydrogen permeation parameters of X52 pipeline steel in wet H_2S environment at various temperatures. The partial pressure of H_2S is 0.1 MPa.

T, °C	Weight loss, g	H_{total}, mmol	J_{total} ×10^{-11}mol/cm^2/s	J_∞, ×10^{-11}mol/cm^2/s	J_∞/J_{total}, %
30	0.0747	2.67	983.38	44.39	4.51
35	0.1794	6.41	2361.68	57.45	2.43
40	0.092	3.29	1211.12	74.97	6.19

The calculated values are listed in Table 4. J_∞/J_{total}, which represents the ratio of permeated hydrogen atoms to the generated hydrogen atoms, can be taken as the measurement of the inhibition effect of the corrosion product film. At 35°C, with the smallest J_∞/J_{total}, the corrosion product film had a best inhibition effect for hydrogen permeation, while at 40°C the inhibition effect was the worst. This result can be explained by the characteristic of the surface morphology.

3.3 Surface characterization

Fig.5 shows the SEM images of the corrosion products formed in wet H_2S environments at different temperatures. Fig.6 presents the XRD patterns of the corrosion products. As shown in Fig.6, mackinawite was the only corrosion product under wet H_2S condition. This is consistent with the result of Shi [16], who believed that mackinawite mainly formed at low temperatures and low H_2S partial pressures. The presence of Fe peak in the XRD patterns indicated that the corrosion film formed in wet H_2S conditions was thin, further proving that the corrosion scale was less protective. The result is in accordance with that of Zhou [8]. At 30°C, a two-dimensional mackinawite layer was partially deposited on the sample surface, and small cracks were found, assumed to be formed as a result of dehydration. At 35°C and 40°C, the sample surface was covered by grain-shaped mackinawite, while dissolved mackinawite was only found at 40°C.

At 30°C, the low permeation rate was restricted by the corrosion rate and deposited mackinawite. As temperature increased to 35°C, at which the corrosion rate was the largest, more hydrogen atoms were generated. In contrast, the corrosion products were denser in comparison with those formed at 30 and 40°C. This would make hydrogen permeation difficult. At 40°C the corrosion products were partial dissolved. Dissolved mackinawite then became a gallery for hydrogen atoms to enter into the steel. Therefore, though the corrosion rate showed a peak value at 35°C, the permeation rate was still lower than that at 40°C.

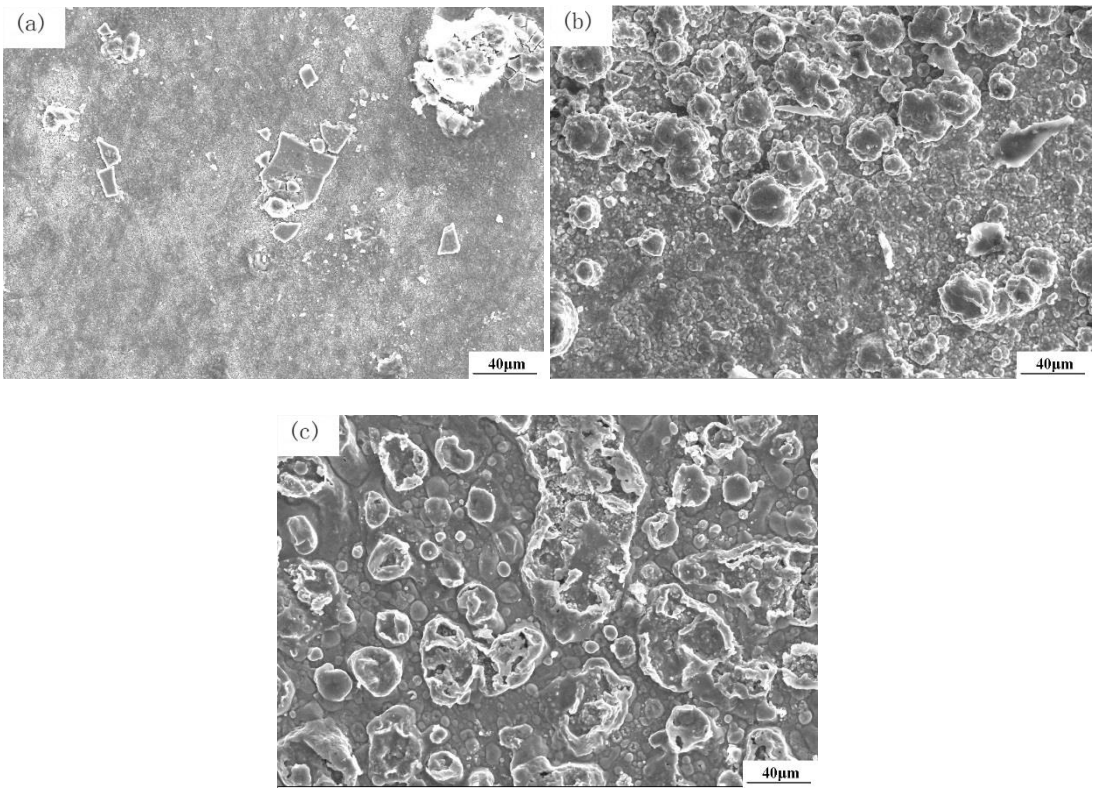

Figure 5. SEM micrographs of the corrosion products formed after exposure to wet H_2S environments at various temperatures: (a) 30°C; (b) 35°C; (c) 40°C. The partial pressure of H_2S is 0.1 MPa.

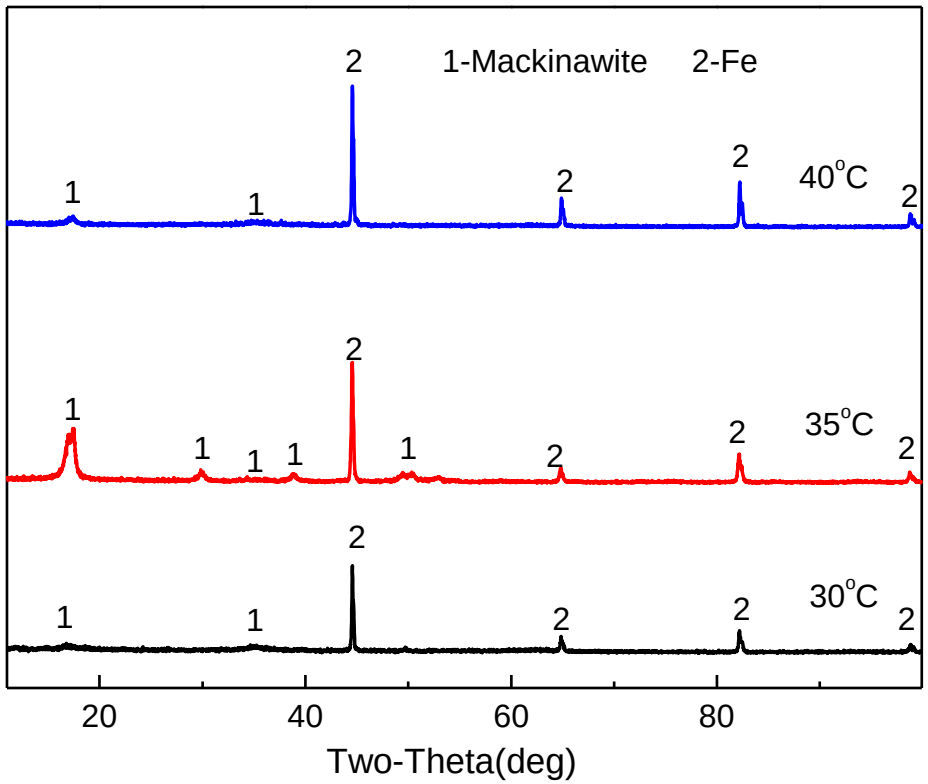

Figure 6. XRD patterns of corrosion products formed after exposure to wet H_2S environments at various temperatures: (a) 30°C; (b) 35°C; (c) 40°C. The partial pressure of H_2S is 0.1 MPa.

4. CONCLUSION

In the present work, the effect of temperature on the permeation behavior of pipeline steel was investigated in wet H_2S condition by electrochemical tests and immersion tests. The results are summarized as follows:

(1) The steady-state permeation current density, steady-state flux and the permeation rate increased with increasing temperature.

(2) The polarization results indicated that the corrosion process at various temperatures was controlled by the cathodic reaction. Both the electrochemical and immersion tests indicated that the corrosion rate was higher at 35°C.

(3) The hydrogen permeation behavior in wet H_2S condition was affected by the corrosion rate and the corrosion product.

ACKNOWLEDGEMENT
This work was supported by National Natural Science Foundation of China (Grant No. 51271025 and 51371034)

References

1. R. Feng, J. Beck, M. Ziomek-Moroz and S. N. Lvov, *Electrochim. Acta*, 212 (2016) 998.
2. R. Feng, J. Beck, M. Ziomek-Moroz and S. N. Lvov, *Electrochim. Acta*, 241 (2017) 341.
3. Y. Choi, S. Nesic and S. Ling, *Electrochim. Acta*, 56 (2011) 1752.
4. C. Plennevaux, J. Kittel, M. Fregonese, B. Normand, F. Ropital, F. Grosjean and T. Cassagne, *Electrochem. Commun.*, 26 (2013) 17.
5. R. N. Parkins, A review of stress corrosion cracking of high pressure gas pipelines, CORROSION 2000, Orlando, America, 2000, 10
6. D. Masouri, M. Zafari and A. M. Araghi, Sulfide stress cracking of pipeline-case history, CORROSION 2008, New Orleans, America, 2008, 8.
7. C. Zhou, S. Zheng, C. Chen and G. Lu, *Corros. Sci.*, 67 (2013) 184.
8. C. Zhou, X. Chen, Z. Wang, S. Zheng, X. Li and L. Zhang, *Corros. Sci.*, 89 (2014) 30.
9. J. Bockris, D. Drazic and A. R. Despic, *Electrochim. Acta*, 4 (1961) 325.
10. E. J. Kelly, *J. Electrochem. Soc.*, 112 (1965) 124.
11. E. McCafferty and N. Hackerman, *J. Electrochem. Soc.*, 119 (1972) 999.
12. S. Arzola-Peralta, J. Mendoza-Flores, R. Duran-Romero and J. Genesca, *Corros. Eng. Sci. Techn.*, 41 (2006) 321.
13. J. Tang, Y. Shao, J. Guo, T. Zhang, G. Meng and F. Wang, *Corros. Sci.*, 52 (2010) 2050.
14. G. Itoh, K. Koyama and M. Kanno, *Scripta. Mater.*, 35 (1996) 695.
15. G. M. Pressouyre, *Metal. Mater. Trans. A*, 10A (1979) 1571.
16. F. Shi, L. Zhang, J. Yang, M. Lu, J. Ding and H. Li, *Corros. Sci.*, 102 (2016) 103.